Ocean Dynamics (2012) 62:253–264
DOI 10.1007/s10236-011-0499-z

Classification of acoustically stable areas using empirical orthogonal functions

Karl Thomas Hjelmervik · Jan Kristian Jensen · Petter Østenstad · Atle Ommundsen

Received: 10 December 2010 / Accepted: 21 September 2011 / Published online: 11 November 2011

Abstract Sonar performance modeling is crucial for submarine and anti–submarine operations. The validity of sonar performance models is generally limited by environmental uncertainty, and particularly uncertainty in the vertical sound speed profile (SSP). Rapid environmental assessment (REA) products, such as oceanographic surveys and ocean models may be used to reduce this uncertainty prior to sonar operations. Empirical orthogonal functions (EOF) applied on the SSPs inherently take into account the vertical gradients and therefore the acoustic properties. We present a method that employs EOFs and a grouping algorithm to divide a large group of SSPs from an ocean model simulation into smaller groups with similar SSP characteristics. Such groups are henceforth called acoustically stable groups. Each group represents a subset in space and time within the ocean model domain. Regions with low acoustic variability contain large and geographically contiguous acoustically stable groups. In contrast, small or fragmented acoustically stable groups are found in regions with high acoustic variability. The main output is a map of the group distribution. This is a REA product in itself, but the map may also be used as a planning aid for REA survey missions.

Responsible Editor: John Osler

This article is part of the Topical Collection on *Maritime Rapid Environmental Assessment*

K. T. Hjelmervik (✉) · J. K. Jensen · P. Østenstad · A. Ommundsen
Norwegian Defense Research Establishment (FFI),
P O Box 115, NO-3191, Horten, Norway
e-mail: karl-thomas.hjelmervik@ffi.no

Keywords Ocean modeling · Empirical orthogonal functions · Classification · Acoustic modeling

1 Introduction

Environmental uncertainty generally limits the validity of sonar performance models (James and Dowling 2008). In the mid–frequency range (1 to 10 kHz), typically used by anti–submarine warfare (ASW) sonars, uncertainty in sound speed profile (SSP) has significant impact on the modeled transmission loss (Dosso 2003; Dosso et al. 2007; LePage 2006a, b, c; Finette 2006) used in sonar performance predictions. The output of sonar performance models is important when planning the placement of sonar assets during ASW sonar operations. A consequence of uncertainty in predicted sonar range is that more sonar assets are required to obtain the required probability of success. This uncertainty may be reduced by increasing the knowledge of the environment through rapid environmental assessment (REA) missions prior to or during sonar operations. In this context, REA includes different sources of oceanographic information, such as ocean modeling systems or in situ measurements. Although most ocean modeling systems have their deficiencies, their inherent covertness and wide geographical coverage makes them attractive for planning of sonar operations.

The proposed method divides SSPs from an ocean model into smaller acoustically stable groups. The modeled sonar performance, here defined as signal excess (Urick 1983), is approximately the same for all SSPs within an acoustically stable group. Each group represents a subset in space and time of the 4-dimen-

sional ocean model data. The end product is a time series of maps, each map showing the geographical distribution of acoustically stable groups for a single time step. Regions consisting of fragmented or small acoustically stable groups are considered acoustically unstable, while regions consisting of large and contiguous acoustically stable groups are considered acoustically stable.

The method combines empirical orthogonal functions (EOF) (Preisendorfer 1988) and clustering (Jain and Dubes 1988). This is equivalent to methods used on echo sounder data for seabed classification (Milligan et al. 1978). However, the clustering method is computationally expensive. A less refined grouping algorithm, henceforth called the coefficient sign test (CST), with far lower computational cost is proposed and compared to clustering.

The method is tested on SSPs from Westcoast200m (Engedahl 1995), a high resolution numerical ocean model covering 16.000 square kilometers adjacent to the Norwegian coast. This high resolution model provides us with a gridded data set in both space and time where oceanographic dynamical features are realistically resolved.

2 Method

Given a group of SSPs from an ocean model, the group is split into smaller acoustically stable groups by analysing their EOF coefficients (Section 2.1) and using the following algorithm:

1. The algorithm starts with a group of SSPs, and a cost function (Section 2.3), henceforth called the EOF cost function, is used to check if the group can be considered acoustically stable for the given sonar scenario.
   - If the estimated cost of the group is below the selected threshold T_f, the group is accepted as acoustically stable and not further processed. If not, the group is passed on to step 2.
2. A grouping algorithm (Section 2.2) splits the group into two smaller groups. In this study we compare two grouping algorithms, both based on analysis of EOF coefficients.
   - Groups with less than K SSPs are considered too small and are therefore removed. The remaining groups are used as input to the next iteration (step 1).

The size limitation, given by K, dictates the minimum geographical coverage of the acoustically stable groups. The preferred minimum size depends on the application. Without the size requirement the analysis would include a large number of tiny, but acoustically stable groups — in extreme cases, one group could theoretically contain only a single profile. Groups that do not meet the size limitation are allocated to a single group that is considered acoustically unstable, typically plotted in grey, Section 4.

Note that the group of SSPs considered may extend in time as well as space. In that case, the acoustically stable groups extend both in space and time. One of the main advantages by including time–dependent ocean model data is that the geographical extent of a particular type of water mass, represented by an acoustically stable group, may be tracked through time.

2.1 Empirical orthogonal functions

A detailed account on how EOFs are derived from a data set is found in Preisendorfer (1988). The following gives a short synopsis of the method.

Consider a data matrix $\widehat{\mathbf{C}}$, where each row contains a single mean subtracted SSP, $\widehat{\mathbf{c}}(\mathbf{x}, t)^T$ with an associated position, $\mathbf{x}$, and time, t. The mean subtracted SSP is given by:

$$\widehat{\mathbf{c}} = \mathbf{c} - \bar{\mathbf{c}} \tag{1}$$

where $\mathbf{c}$ is a SSP and

$$\bar{\mathbf{c}} = \frac{1}{M}\sum_{m=1}^{M} \mathbf{c_m}, \tag{2}$$

where $\mathbf{c_m}$ is the mth SSP.

The correlation matrix, $\mathbf{R_C}$ is given by:

$$\mathbf{R_C} = \frac{1}{M}\widehat{\mathbf{C}}^T\widehat{\mathbf{C}}, \tag{3}$$

where M is the number of SSPs in the data matrix. The SSPs may then be represented by the following expression:

$$\mathbf{c} = \bar{\mathbf{c}} + \sum_{k=1}^{N} \kappa_k \mathbf{u_k}, \tag{4}$$

where $\mathbf{u_k}$ are EOFs and may be derived by solving the following eigenvector problem:

$$\mathbf{R_C u_k} = \lambda_k \mathbf{u_k}, \tag{5}$$

where λ_k is the eigenvalue corresponding to $\mathbf{u_k}$. There are N EOFs, where N is the number of depth steps in the SSPs. The EOF corresponding to the highest eigenvalue is commonly called the leading coefficient.

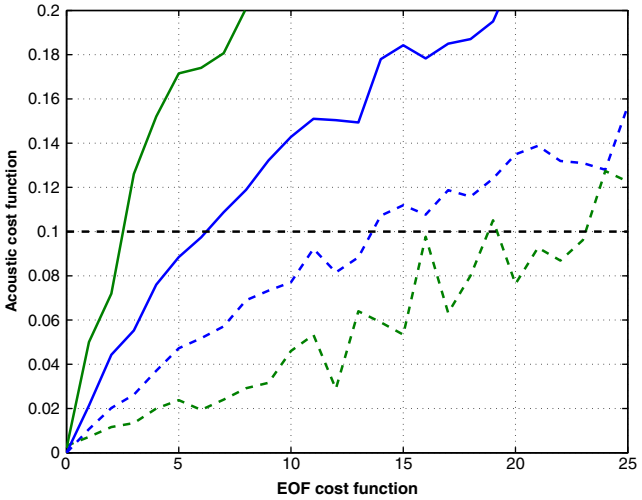

Fig. 1 Comparison of the EOF cost function to the acoustic cost function for the two sonars and two data sets considered. The *dashed line* indicates the limit used on the acoustic cost function to determine whether a group has stable sonar conditions

The coefficients, κ_k, representing a specific SSP, $\widehat{c}$, are found as follows:

$$\kappa_k = \mathbf{u_k}^T \widehat{\mathbf{c}}. \tag{6}$$

2.2 Grouping of sound speed profiles

Two different algorithms for splitting a group of SSPs into two smaller groups are presented. The first is a conventional clustering algorithm (CA) while the second, henceforth called coefficient sign test (CST) is a less refined algorithm developed for low computational cost and for managing large data sets.

Cluster analysis (Jain and Dubes 1988) is assigning data points with similar characteristics to the same group of data, called a cluster. The CA employs hierarchical clustering on the five leading EOF coefficients with the Euclidean distance function and cluster average midpoint to calculate the distance between clusters (Jain and Dubes 1988). SSPs with similar vertical structure are close together in coefficient space — and will be assigned to the same cluster.

The coefficient sign test applies an EOF analysis on the input group of SSPs. The SSPs are subsequently split in two groups; one where the leading coefficient is positive and one where the leading coefficient is negative. Note that due to the iterative main algorithm, both the EOF analysis and the subsequent splitting is done on progressively smaller subsets of the original data set.

Table 1 Thresholds on the EOF cost function for different sonars and data sets

	March 2007		June 2010	
	HMS	TAS	HMS	TAS
Threshold	7	13	3	23

2.3 Cost function

The EOF cost function used to assess the acoustic stability of a group is simply the summed variances of the coefficients representing the SSPs in that group. Consider a group of N SSPs represented by EOF coefficients. The cost, f, is given by:

$$f = \sum_{k=1}^{N} \mathrm{Var}(\kappa_k). \tag{7}$$

The variance of the coefficients, $\mathrm{Var}(\kappa_k)$, is given by:

$$\mathrm{Var}(\kappa_k) = \frac{1}{N-1} \sum_{j=1}^{N} \left(\kappa_k^{(j)} - m_k\right)^2, \tag{8}$$

where

$$m_k = \frac{1}{N} \sum_{j=1}^{N} \kappa_k^{(j)} \tag{9}$$

and $\kappa_k^{(j)}$ is the kth coefficient representing the jth SSP in that group. If the cost is below a set threshold, T_f, then that group is considered acoustically stable. Note that f is equivalent to the summed depth dependent variance of all SSPs in the group.

The main intent of the presented method is to divide a large geographical area into smaller areas with stable sonar conditions. The EOF cost function is based on an EOF analysis of the SSPs contained in that area and therefore efficiently captures oceanographic variations. However, there is not a linear relationship between the sonar conditions and these variations. Also, the sensitivity of the sonar conditions to oceanographic variations depends on the present sonar–target geometry (Kessel 1999; Hjelmervik and Sandsmark 2008).

The following analysis is included in order to assess the quality of the EOF cost function. The EOF cost function is compared to an acoustic cost function. The acoustic model Lybin (Hjelmervik et al. 2008) is used to estimate the signal excess for each SSP contained in the analysed area.

The performances of two different active sonars are estimated; a hull mounted sonar (HMS) at 5 m depth and a towed array sonar (TAS) at 100 m depth. Two different sonars are used in order to demonstrate that

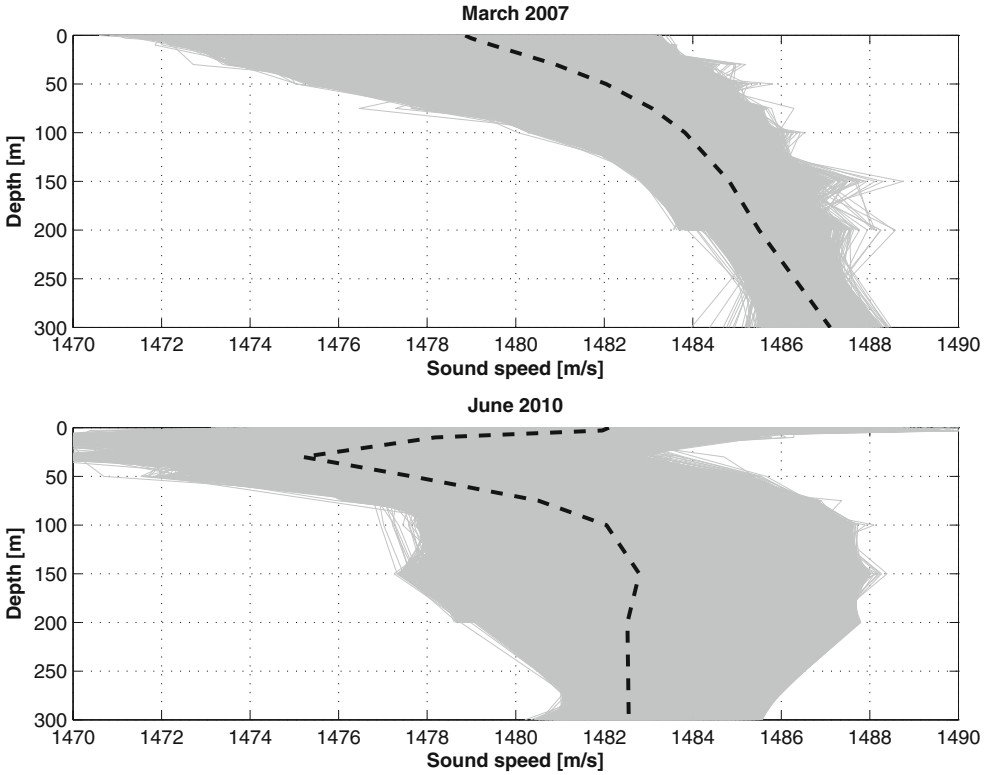

Fig. 2 SSPs for both the March 2007 (*top*) and June 2010 (*bottom*) data set. The *black dashed line* represents the average SSP

the threshold applied on the EOF cost function should depend on the sonar used, and particularly the depth of the sonar used.

A flat bottom at 300 m depth is assumed. A generic group of SSPs are generated by selecting a random set of Gaussian distributed EOF coefficients, where the

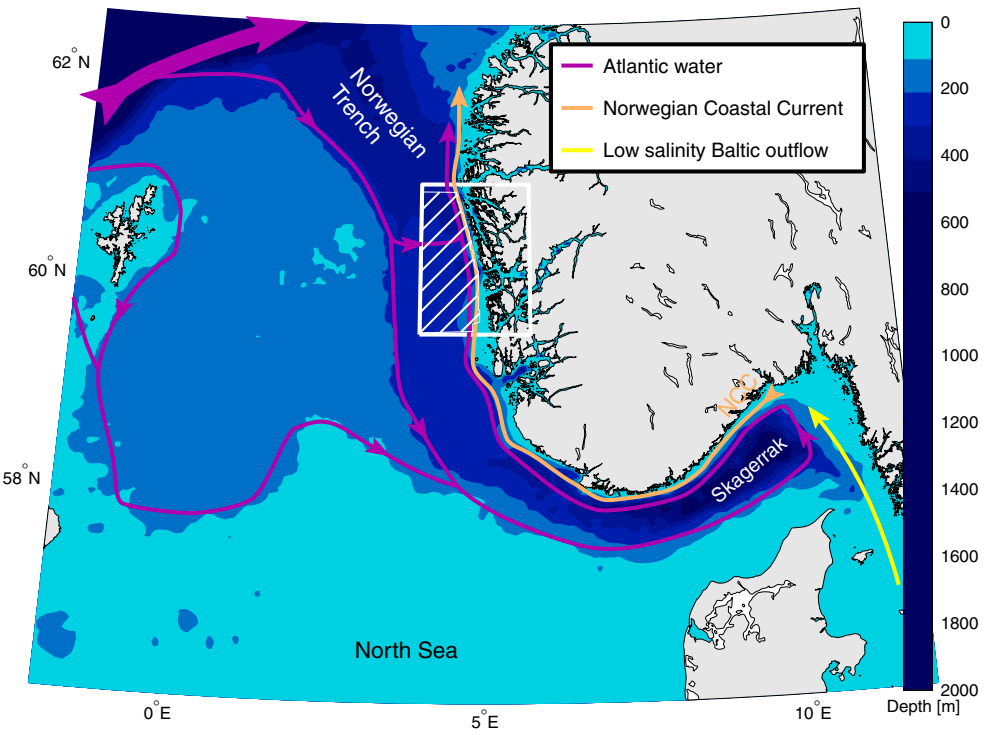

Fig. 3 Basic oceanographic circulation patterns of the northern North Sea. Note that wind effects and mesoscale dynamics cause considerable variations to the location of the currents, including meanders and eddy formation. The *white box* shows the domain of the ocean model, whereas the *white hatched area* indicates the domain of the data used after removal of data points in fjord inlets and in areas shallower than 200 meters

summed coefficient variances are varied from 0 to 25. Note that the sum of the coefficient variances is equal to the value of the EOF cost function for that group of SSPs. The EOFs and the ratio of the eigenvalues and the leading eigenvalue are derived from the data sets presented in Section 3.

The acoustic cost function is simply the averaged percentage of target ranges, r, and depths, z, considered where the bias, b, exceeds a set threshold, T. The averaging is over all SSPs in that group. The bias for a single SSP is defined as:

$$b(r,z) = \left| SE_j(r,z) - SE_m(r,z) \right|, \tag{10}$$

where $SE_j(r,z)$ is the modeled signal excess at $[r,z]$ using the jth SSP in the acoustic model. The mean signal excess, $SE_m(r,z)$, is given by:

$$SE_m(r,z) = 10\log_{10}\frac{1}{N}\sum_{j=1}^{N} 10^{SE_j(r,z)/10}, \tag{11}$$

where N is the amount of SSPs in the considered group. Groups where the computed percentage is below a selected limit are assumed to have stable sonar conditions. Here we consider 0.1 to be an appropriate limit.

Figure 1 shows the acoustic cost function versus the EOF cost function for the HMS and TAS for each data set. A threshold, T, of 5 dB and target ranges of 2 km to 10 km and depths of 10 m to 200 m are considered when estimating the acoustic cost function. The acoustic cost function clearly increases when the EOF cost function increases for both sonars in both data sets. However, the relationship between the cost functions is different for different sonars and data sets. This clearly shows that the threshold used on the EOF cost function when determining what groups are stable should depend on the sonar used and on the data set considered. The comparison between the two cost functions should therefore be made prior to any analysis to ensure that the threshold used complies with any requirements on acoustic stability. Thresholds on the EOF cost function that correspond to an acoustic cost of 0.1 (Fig. 1) were chosen and are listed in Table 1.

3 Example area and data set

The study area is in the North Sea, close to the western coast of Norway (Fig. 3). This part of the North Sea is relatively flat, with depths around 300 m, with a steep rise at the Norwegian Coast to the east. Circulation in the area is dominated by inflow and recirculation of saline Atlantic water (AW) which enters the North

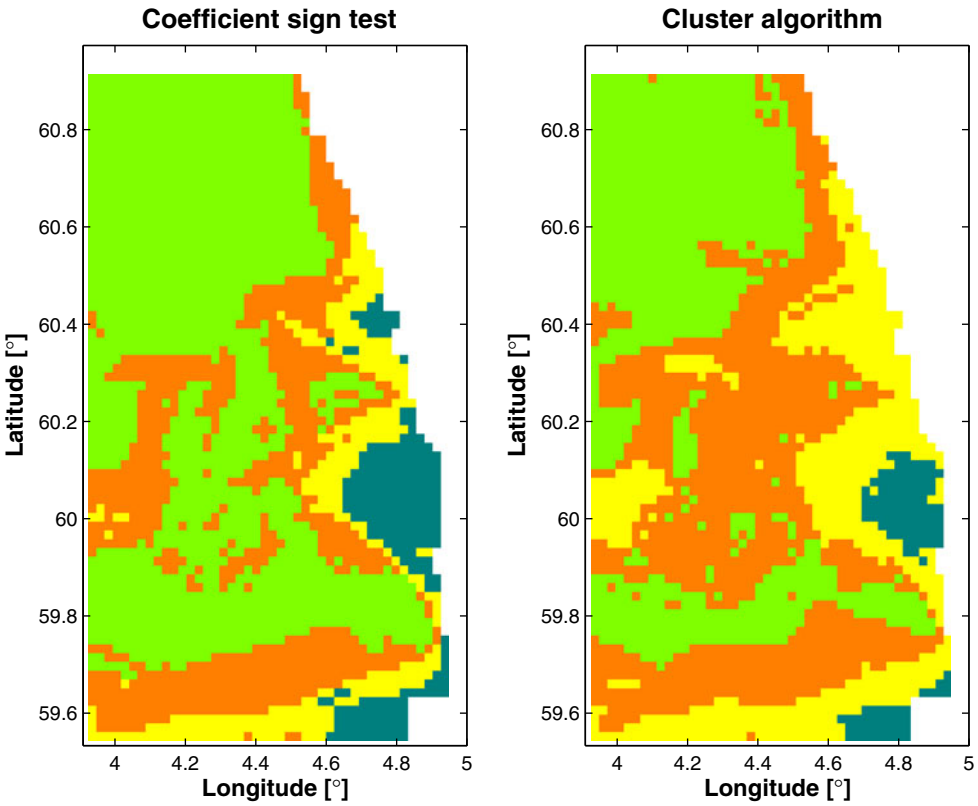

Fig. 4 Comparison of group distributions when using the two different grouping algorithms on data from a single time step of a downsampled version of the March 2007 data set (03-Mar-2007 12:00:00 UTC). The threshold corresponding to the HMS sonar is used, see table 1

Sea from the north and the low salinity coastal waters (CW) in the Norwegian Coastal Current (NCC) (Fig. 3) (Svendsen et al. 1991; Otto et al. 1990; Winter and Johannessen 2006). The NCC originates in Skagerrak as very low salinity water from the Baltic and is mixed with the water of the North Sea. The latter is essentially of Atlantic origin, but more or less diluted (freshened) through its residence in the North Sea (Svendsen et al. 1991; Otto et al. 1990). The NCC follows the Norwegian coast, but with variable lateral extent which is mainly controlled by wind forcing and meander/eddy formation processes. The usual features of frontal dynamics (frontal structures, filaments, meanders and eddies) are found at the transition between coastal and Atlantic water masses (Svendsen et al. 1991; Johannessen et al. 1989). In general water masses with salinity greater than 35 psu are referred to as AW and below 35 psu as CW (Otto et al. 1990).

The SSPs (Fig. 2) used in this study are based on three dimensional forecasts of temperature and salinity from the high resolution numerical ocean model Westcoast200m. This ocean model is a version of Princeton Ocean Model (POM) (Engedahl 1995; Ommundsen et al. 2008), run operationally by the Norwegian Meteorological Institute. The model domain covers an area of approximately 16.000 km^2, from 59.30° N 4° E to 61° N 5.75° E with a horizontal resolution of 200 m (white box in Fig. 3). The forecast period is 33 hours with 11 time steps at 3 hour intervals. The data are subsampled to a horizontal resolution of approximately 1 km, 11 time steps (3 hours), and 9 depth levels ranging from 0 to 200 m. Most data from fjords and inlets are removed, as well as all points shallower than 200 meters. The white hatched area (Fig. 3) shows the extent of the area considered after removal of shallow water and fjord inlet data points.

Two periods are studied, March 2–3 2007 and June 4–5 2010, and each data set consists of 110.363 profiles distributed over the eleven time steps.

In March, there is a strong correlation between water temperature and salinity, with CW being cold and fresh and AW being higher in temperature and salinity. The

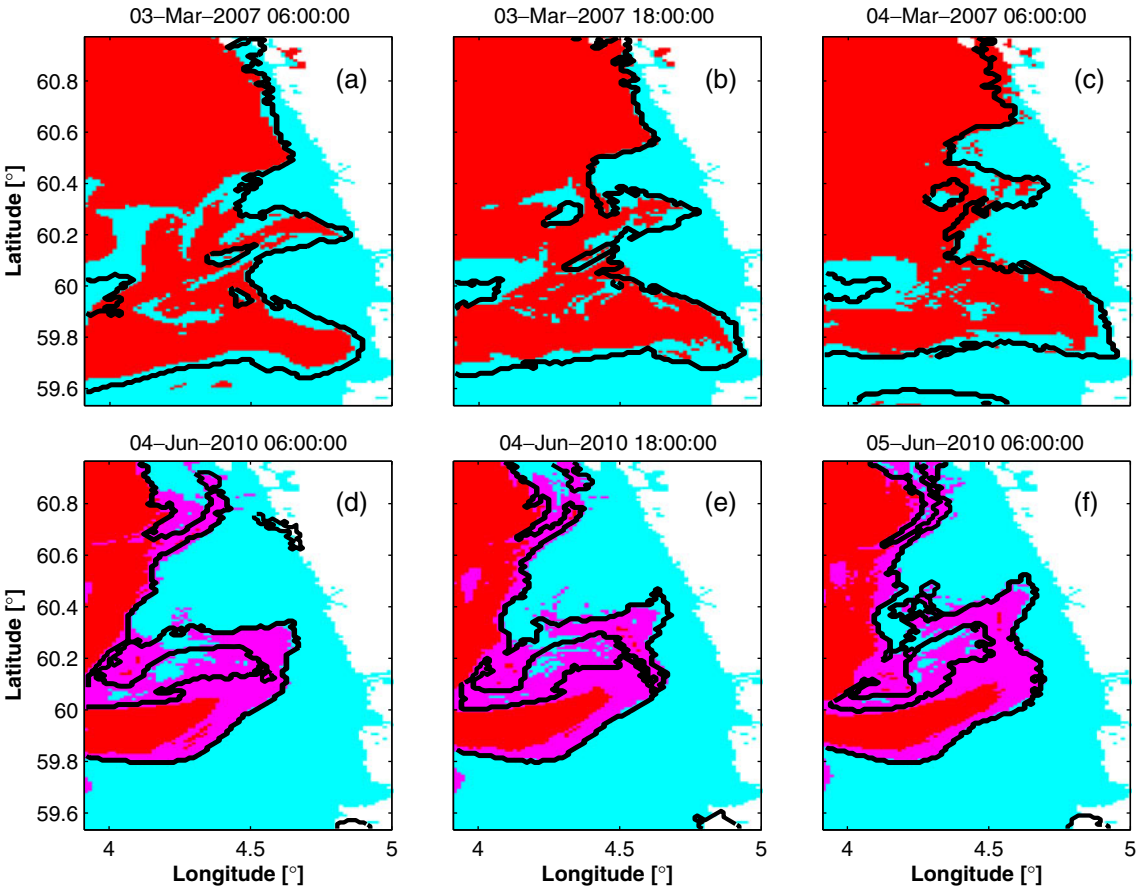

Fig. 5 The distribution of groups when using the TAS for three different time steps of the March 2007 data set (**a**–**c**) and the June 2010 data set (**d**–**f**). The plots are ordered chronologically from left to right with 12 hour between each time step. The *black lines* indicate the 35 psu salinity contours at 50 m depth for the March 2007 data set and 100 m depth for the June 2010 data set

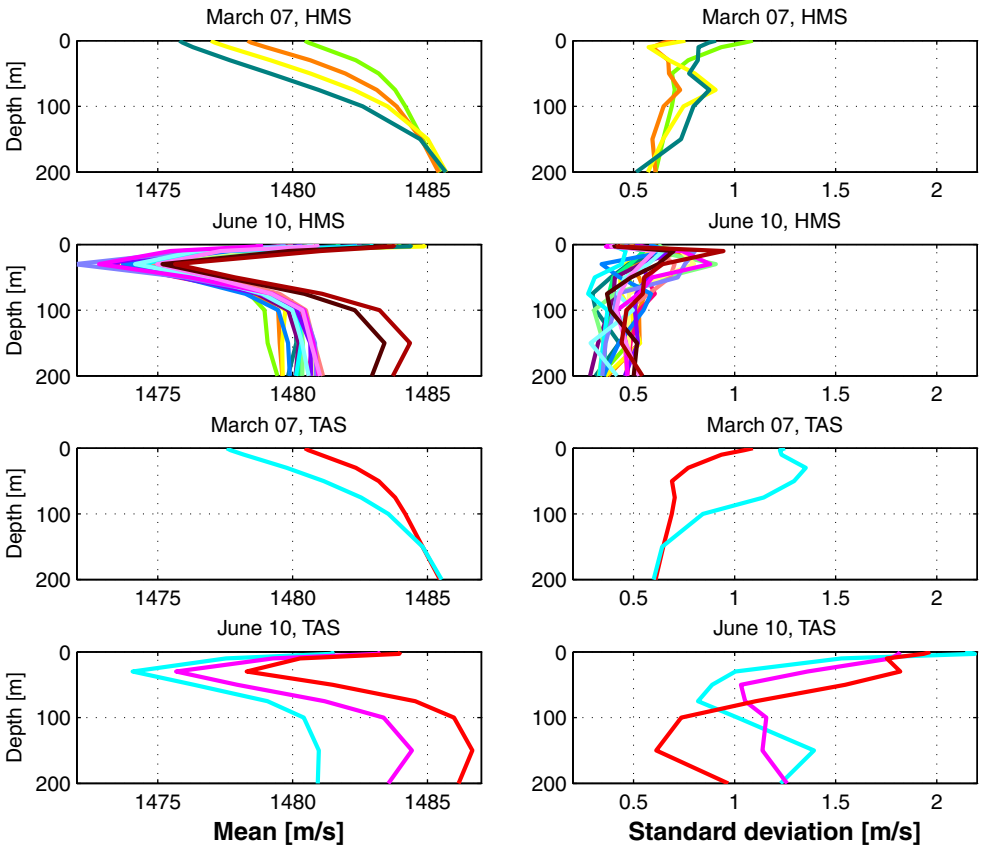

Fig. 6 The mean SSPs (*left*) and their standard deviation (*right*) as a function of depth for each acoustically stable group of SSPs. The *colors* correspond to the colors of the group distributions shown in Figs. 5 and 10

typical distribution of the two water masses is that the CW is wedged between the Norwegian coast and the adjacent AW, the deepest part of CW being close to the coast. The exact location of the transition zone between the two water masses is highly variable due to mesoscale dynamics.

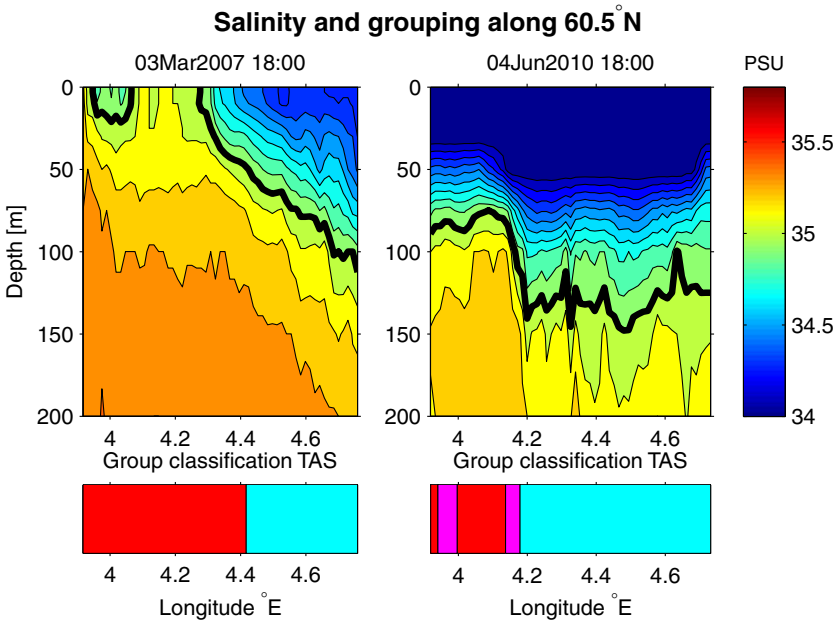

Fig. 7 Vertical section of salinity (*upper panels*) along 60.5° N for 3 March 2007 18 UTC (*left panels*) and 4 June 2010 18 UTC (*right panel*). The *thick black line* indicates the 35 PSU salinity contour. The corresponding group distribution for the TAS sonar scenario is shown in the *lower panels*. The data correspond to panel (**b**) and (**e**) of Fig. 5. Note that the color scale does not represent the full dynamic range of the salinity values for June 2010 – the actual salinity minimum is close to 31 psu

In June the CW is less saline due to increased fresh water input from the Baltic and rivers along the North Sea and Skagerrak coasts. Along with higher surface temperature the NCC has strong vertical sound speed gradients in the near surface layers (Fig. 2). The distribution of the CW and AW is also different than in March: due to a reduction in the south westerly wind field and more prevailing northerly winds during summer, the coastal current becomes wider and shallower. Usually a layer of CW overlays the AW for the major part of our study area (Sætre et al. 1988).

4 Results and discussion

The proposed method is demonstrated on the data sets described in the previous section. Two different sonars are considered; a hull–mounted sonar and a towed array sonar. As stated in Section 2.3 different thresholds on the cost function are used for different data sets and sonar systems (Table 1). The lower group size threshold (step two of the overall algorithm in Section 2) was chosen to be $K = 500$ SSPs. A group consisting of 500 SSPs approximately covers a geographical area of 45 km^2 on average over eleven timesteps. Such small sized groups typically appear in unstable regions between larger groups, and are therefore discarded from the analysis and collected in a single acoustically unstable group such as the grey group in Fig. 10.

Figure 4 shows a comparison of the distributions of stable groups when using CA and CST methods on a downsampled version for a single time step of the March 2007 data set presented in Section 3. This downsampled data set contains 2833 SSPs, or 28% of the full data set for a single time step (10.033 profiles). The CA method is very demanding in terms of computer memory, and the 2833 data set is close to the memory limitation on our computers. Both methods generate four groups. Notice how well the two methods compare in the northern and southern part of the ocean model domain. The main differences are found in the unstable center region. In the remaining analyses the CST algorithm is used on the full data sets.

Figure 5 shows the group distribution for selected time steps in the March 2007 and June 2010 data sets when using TAS. The vertical mean SSPs for each group as well as their standard deviations are shown in Fig. 6. Three groups are needed in the June 2010 data set to meet the requirements for stability, as opposed to two groups in the March 2007 data set. The contour lines of the 35 psu salinity value at the selected depths (Fig. 5) coincide remarkably well with the group distribution. In the literature, the 35 psu salinity value is considered a good choice for separating CW and AW (Section 3 and Otto et al. (1990)). However, the full three dimensional structure should be considered. Figure 7 shows a vertical cross-section of the salinity and the group distribution for TAS along an

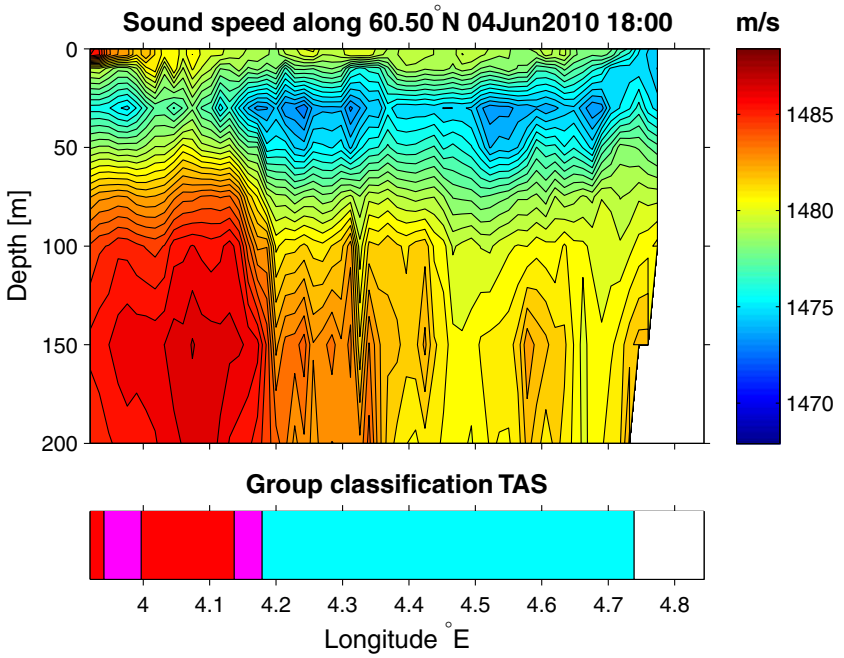

Fig. 8 Vertical section of sound speed (*upper panel*) along 60.5° N for 4. June 2010 18 UTC and the corresponding group distribution for TAS sonar scenario (*lower panel*). The data corresponds to panel (**e**) of Fig 5

east–west line at 60.5° N for March 3, 2007 18 UTC (left panel), which corresponds to panel (b) of Fig. 5. The low salinity CW adjacent to the coast has the classical wedge–shaped structure overlaying the saltier AW, a distribution typical for the winter season in this area. In the winter, temperature, sound speed and salinity are well correlated. The red group therefore represents conditions with little or no CW in the upper layers and AW more or less through the entire water column. In contrast, the cyan group is dominated by CW overlaying saltier AW, corresponding to increased vertical sound speed gradients, as is clearly seen in Fig. 6.

The June 2010 data (Fig. 7, right panel) is dominated by CW overlaying AW throughout the entire area of investigation, but at markedly deeper depths in the eastern and center part, corresponding to the cyan group. The 35 psu line is around 80 m west of 4.2° E and at 120–140 m eastward of 4.2° E, with a very steep gradient close to this longitude. However, the depth of the transition between AW and CW is not enough to explain the classification. In June, the correlation between temperature and salinity is less straightforward than in the winter due to surface heating. Figure 8 shows a marked sound speed minimum centered around 30 m throughout the entire cross section along 60.5° N. This minimum is markedly stronger eastward of 4.2° E. Most likely, it is the combination of a more pronounced sound speed minimum at 30 m and a deeper transition (∼ 120–140 m versus ∼ 80 m) between CW and AW that influences the classification of the cyan versus the red and pink groups.

Notice how groups shown in Fig. 5 propagate and reshape as time elapses. Since data from all time steps are used in a single analysis, the groups are calculated as a function of time as well as position. The motions of the water masses are therefore automatically taken into account and the groups are efficiently tracked through time. For both data sets there is typically movement northward which complies well with what is observed in Fig. 9, where depth–averaged currents are overlain on

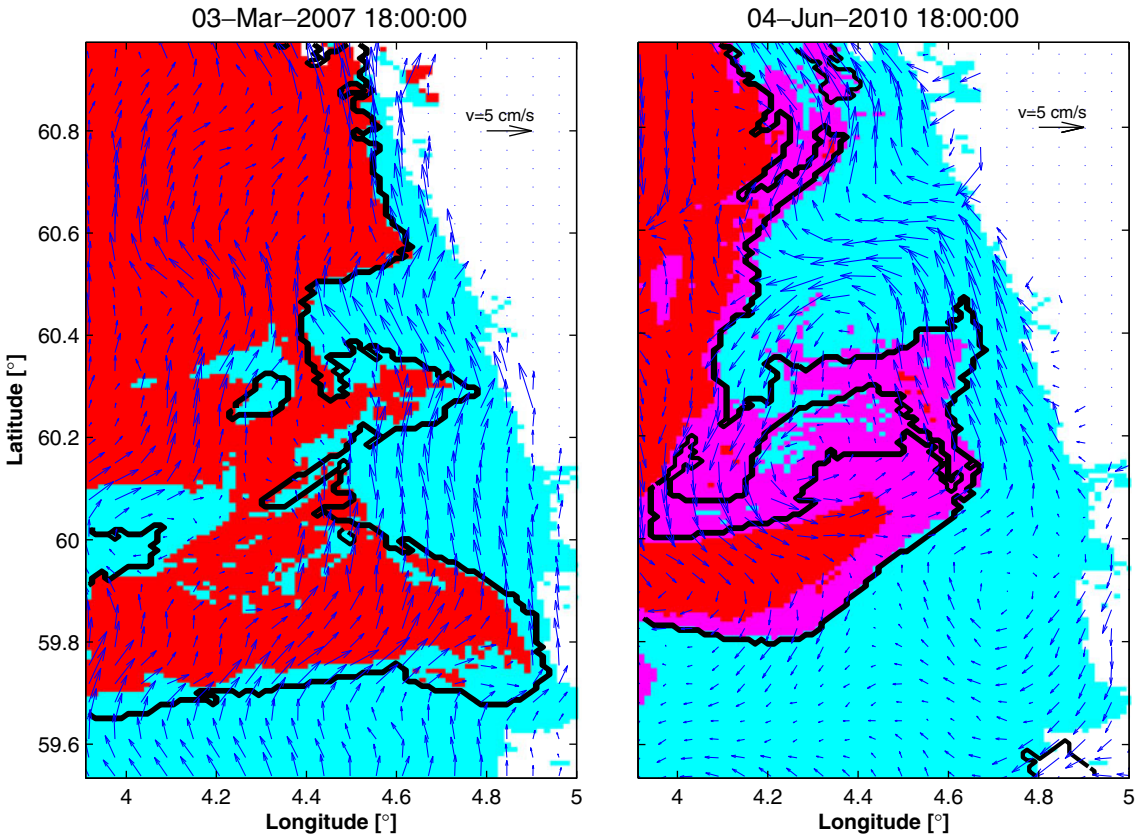

Fig. 9 The distribution of groups when using the TAS for the March 2007 data set (*left*) and the June 2010 data set (*right*) for the time steps shown in Fig. 5 panels (**b**) and (**e**). The *black lines* indicate the 35 psu salinity contours at 50 m depth for the March 2007 data set and 100 m depth for the June 2010 data set. The *arrows* show the direction of the depth–averaged currents

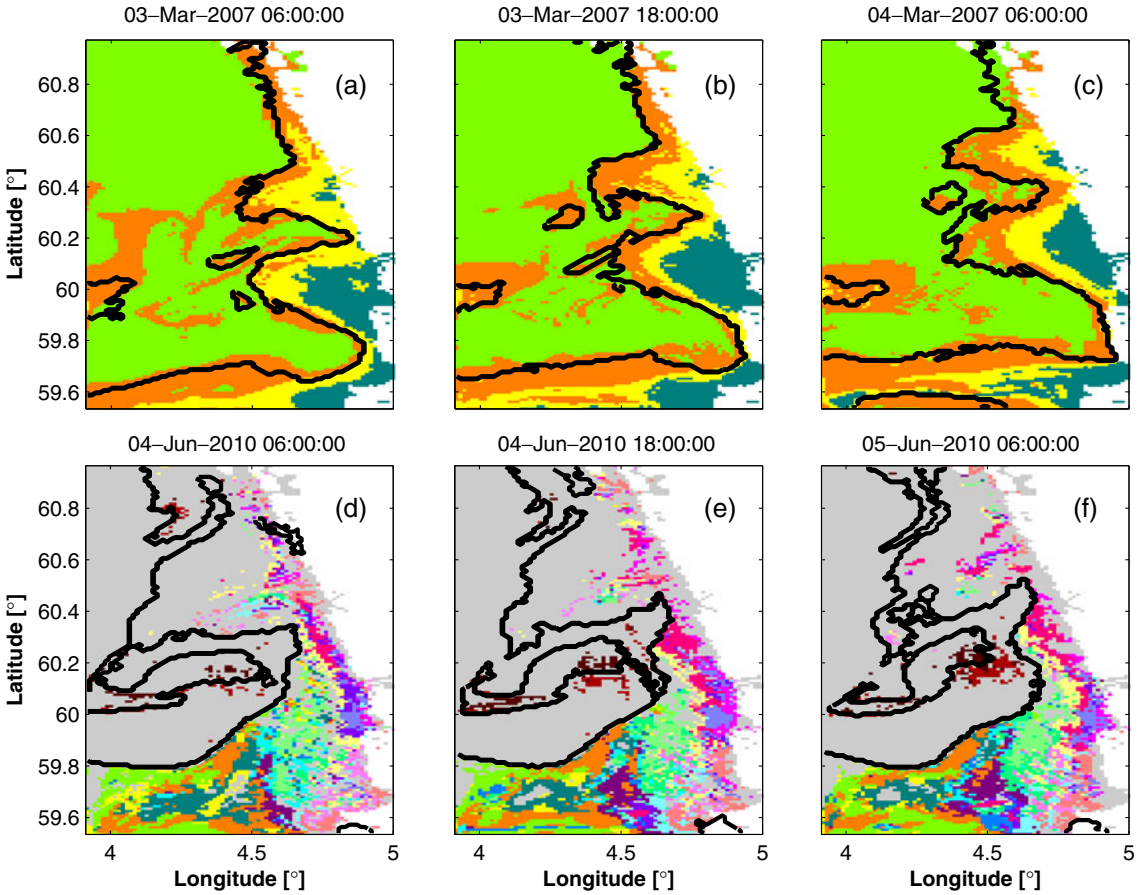

Fig. 10 These plots are equivalent to Fig. 5 but are for the HMS instead of the TAS. The large grey group consists of a large amount of smaller groups that do not meet the minimum size criteria, see Section 2

the group structure. Notice that for the June 2010 data set, the pink group is wedged between the two other groups and the extent of the pink group is largest where there is greatest interaction between the red and cyan groups, e.g. in the centre of the area where an eddy is present (approximately at 60.2° N and 4.4° E).

Figure 10 shows the group distribution for selected time steps in both data sets when using the HMS. The vertical mean SSPs for each group as well as their standard deviations are shown in Fig. 6. The grey colored area in the June 2010 data set represents (panel d through f) a large number of very small groups (less than 500 SSPs in total over all time steps). The different colors indicate the individual acoustically stable groups that exceed the minimum size criteria. It is next to impossible to find any large contiguous acoustically stable region, which indicates that the sonar conditions are very unstable for an HMS in the June 2010 data set. This is due to the presence of very strong and variable sound speed gradients in the upper 20 m of the water column, where the HMS is located. The March 2007 data set results in the generation of four groups with a distribution very similar to the results for the TAS; the orange, yellow, and blue groups combined cover approximately the same area as the cyan group in the TAS case.

5 Summary

The presented method combines analysis of empirical orthogonal functions with grouping algorithms to divide a set of sound speed profiles into smaller, acoustically stable groups. The cost function used to determine acoustic stability, is calibrated for two different sonars; a towed array sonar and a hull mounted sonar. Two different grouping algorithms are compared. The first is a conventional, computationally expensive clustering algorithm. The second is a newly developed, less refined, but more efficient grouping algorithm

called coefficient sign test. The two algorithms produce similar results.

The method using the coefficient sign test grouping algorithm was tested on two different data sets obtained from an ocean model covering an area of approximately 100 km by 160 km area on the western coast of Norway. The first data set is from March 2007, the second from June 2010. The data sets total 110 363 sound speed profiles distributed over 11 different time steps. The method processed the data in less than a minute on a standard desktop computer.

The geographical extent and distribution of the groups were observed to correlate well with the horizontal and vertical distribution of coastal and Atlantic water masses. The exception was the June 2010 data set when using a hull-mounted sonar, which resulted in a very large number of small groups with a speckled, non–contiguous distribution. In June in the North Sea, the seasonal heating of the surface layer has created a pronounced surface duct, and the HMS sonar – being located at 5 m depth – is particularly sensitive to minor variations in the height and strength of this surface duct.

The method produces a map of the group distribution, which is a good indicator of the present acoustic variability. This information is useful in several applications. In REA survey missions, e.g. using gliders, such maps may be used to determine the distribution of assets. For instance, gliders should be concentrated in unstable regions, while stable regions should be well mapped by only a single or a few gliders. The map is also a REA product in itself as a planning aid for sonar operations. For example, during sonar operations the map may be used to determine how often the sonar vessel should measure the sound speed profile; more often in unstable regions than in stable regions.

The spatiotemporal oceanographic variations are typically large in an acoustically unstable region, since the sound speed variance is essentially what the EOF cost function measures. The proposed method may be used to determine for how long a time and for how large an area a measured profile is applicable when modelling sonar performance. Typically, a measured sound speed profile is representative of a smaller area and time in an acoustically unstable region than in a stable region, and thus the sound speed must be measured more densely in space and time in ustable regions.

Depending on the sonar detection range, the sonar coverage may cross several different acoustically stable groups. In such cases a range dependent sound speed profile should be used in sonar performance predictions. If a range dependent sound speed profile is not available, then sonar performance predictions should be considered to have increased uncertainty at ranges that extend into neighbouring areas containing different acoustically stable groups. The use of REA assets before or during sonar operation, may provide range dependent sound speed profiles, and the proposed method may help determine how the available REA assets should be distributed to ensure the collection of range dependent data in acoustically unstable regions.

References

Dosso SE (2003) Environmental uncertainty in ocean acoustic source localization. Inverse Probl 2:419–432. doi:10.1088/0266-5611/19/2/311

Dosso SE, Giles PM, Brooke GH, McCammon DF, Pecknold S, Hines PC (2007) Linear and nonlinear measures of ocean acoustic environmental sensitivity. J Acoust Soc Am 121(1):42–45. doi:10.1121/1.2382719

Engedahl HA (1995) Implementation of the Princeton Ocean Model (pom/ecom3d) at the Norwegian Meterological Institute. DNMI Research Report 5, Norwegian Meteorological Institute, Oslo, Norway

Finette S (2006) A stochastic representation of environmental uncertainty and its coupling to acoustic wave propagation in ocean waveguides. J Acoust Soc Am 120(5):2567–2579. do10.1121/1.2335425

Hjelmervik KT, Sandsmark G (2008) In ocean evaluation of low frequency active sonar systems. In: Proceedings of Acoustics08 (Paris)

Hjelmervik KT, Dombestein EM, Mjølsnes S, Såstad TS, Wegge J (2008) The acoustic raytrace model lybin – description and application. In: Proceedings from Underwater Defence Technology Conference and Exhibition, Glasgow 2008

Jain AK, Dubes RC (1988) Algorithms for Clustering Data. Prentice Hall Advanced Reference Series, Prentice Hall

James KR, Dowling DR (2008) A method for approximating acoustic–field–amplitude uncertainty caused by environmental uncertainties. J Acoust Soc Am 124:1465–1476

Johannessen JA, Svendsen E, Sandven S, Johannessen OM, Lygre K (1989) Three–Dimensional Structure of Mesoscale Eddies in the Norwegian Coastal Current. J Phys Oceanogr 19:3–19

Kessel RT (1999) A mode-based measure of field sensitivity to geoacoustic parameters in weakly range-dependent environments. J Acoust Soc Am 105(1):122–129

LePage K (2006a) Estimation of Acoustic Propagation Uncertainty Through Polynomial Chaos Expansions. In: 9th International Conference on Information Fusion

LePage K (2006b) Modeling Propagation and Reverberation Sensitivity to Oceanographic and Seabed Variability. IEEE J Oceanic Eng 31:402–412. doi:10.1109/JOE.2006.875095

LePage K (2006c) Propagation and Reverberation Sensitivity to Oceanographic and Seabed Variability. IEEE J Oceanic Eng 31(2):402–412. doi:10.1109/JOE.2006.875095

Milligan S, LeBlanc L, Middleton F (1978) Statistical grouping of acoustic reflection profiles. J Acoust Soc Am 64(3):795–807

Ommundsen A, Jensen JK, Midtbø KH, Engedahl H (2008) Operational METOC models at the Norwegian Meteorological Institute. FFI Report 02369, Norwegian Defense Research Establishment (FFI), Kjeller, Norway

Otto L, Zimmerman JTF, Furnes GK, Mork M, Sætre R, Becker G (1990) Review of the physical oceanography of the North Sea. Neth J Sea Res 26:161–238. doi:10.1016/0077-7579(90)90091-T

Preisendorfer RW (1988) Principal Component Analysis in Meteorology and Oceanography. Elsevier, curtis D. Mobley (ed.)

Sætre R, Aure J, Ljøen R (1988) Wind effects on the lateral extension of the Norwegian Coastal Water. Cont Shelf Res 8:239–253. doi:10.1016/0278-4343(88)90031-3

Svendsen E, Sætre R, Mork M (1991) Features of the northern North Sea circulation. Cont Shelf Res 11:493–508

Urick RJ (1983) Principles of underwater sound, 3rd edn. Peninsula Publishing

Winter NG, Johannessen JA (2006) North Sea circulation: Atlantic inflow and its destination. J Geophys Res 111(C12018). doi:10.1029/2005JC003310